

The C-value enigma and timing of the Cambrian explosion

Dirson Jian Li* & Shengli Zhang

Department of Applied Physics, Xi'an Jiaotong University, Xi'an 710049, China

* E-mail: dirson@mail.xjtu.edu.cn.

ABSTRACT

The Cambrian explosion is a grand challenge to science today and involves multidisciplinary study. This event is generally believed as a result of genetic innovations, environmental factors and ecological interactions, even though there are many conflicts on nature and timing of metazoan origins. The crux of the matter is that an entire roadmap of the evolution is missing to discern the biological complexity transition and to evaluate the critical role of the Cambrian explosion in the overall evolutionary context. Here we calculate the time of the Cambrian explosion by an innovative and accurate “C-value clock”; our result (560 million years ago) quite fits the fossil records. We clarify that the intrinsic reason of genome evolution determined the Cambrian explosion. A general formula for evaluating genome size of different species has been found, by which major questions of the C-value enigma can be solved and the genome size evolution can be illustrated. The Cambrian explosion is essentially a major transition of biological complexity, which corresponds to a turning point in genome size evolution. The observed maximum prokaryotic complexity is just a relic of the Cambrian explosion and it is supervised by the maximum information storage capability in the observed universe. Our results open a new prospect of studying metazoan origins and molecular evolution.

INTRODUCTION

The broad outline of Cambrian diversification has been known for more than a century, but only in the post-genomic era have the data necessary to explain the nature of the Cambrian explosion. This problem originated in the disciplines of paleontology and stratigraphy, while the debate about it may be as old as the problem itself [1][2][3]. Some ascribed the Cambrian explosion to intrinsic causes, while others believe that it may have been triggered by environmental factors. Innovative ideas exploded in the past decade with new fossil discoveries and progress in biogeochemistry, molecular systematics and developmental genetics [4][5][6][7]. However, we still need insights from other fields such as genome size evolution, self-organization, complexity theory and the holographic principle [8][9][10][11] to fully resolve this long-running problem.

There is a profound relationship between the Cambrian explosion and the C-value enigma. Why did so many complex creatures appear in the late Neoproterozoic and Cambrian, but not earlier or later? We believe that the nature and timing of the Cambrian explosion can be determined by the evolution of genome size (see the schematic in Supplementary Figure 1). We invented a "C-value clock" to calculate the time of the Cambrian explosion based on genomic data. The basis of the C-value clock depends on the notion that the evolutionary relationship can be revealed by the correlation of protein length distributions and the genome size evolution can be taken as a chronometer.

The start of our theory is a formula for evaluating genome size (namely C-value) of different species. According to this formula, major component questions of the C-value enigma can be solved and the genome size evolution can be illustrated. Consequently, the genome size evolution can be taken as an accurate chronometer to study the macroevolution. We found a unique turning point in genome size evolution and calculated the time of the turning point, which corresponds to the Cambrian explosion. We believe that the Cambrian explosion was es-

entially a major transition of biological complexity when the prokaryotic complexity reached its maximum value. We suggest that the biological complexity is supervised by the maximum information storage capability in the observed universe.

RESULTS AND DISCUSSIONS

Genome size evolution. Genome sizes vary extensively in or between taxa. We found that the genome size S can be determined by two variables: the noncoding DNA content η and the correlation polar angle θ . Hence we obtained an empirical formula of genome size for any contemporary species:

$$S(\eta, \theta) = s_0 \exp\left(\frac{\eta}{a} - \frac{\theta}{b}\right), \quad (1)$$

where $s_0 = 7.96 \times 10^6$ base pairs (bp), $a = 0.165$ and $b = 0.176$ were obtained by least squares based on the data of S , η and θ for 54 species (see Supplementary Table 1 and 2). We also obtained another empirical formula of gene number $N(\eta, \theta) = 1.48 \times 10^4 \exp(\frac{\eta}{0.463} - \frac{\theta}{0.157})$ and the relationship between non-coding DNA and coding DNA for eukaryotes $\log N_{nc} = 2.81 \log N_c - 12.5$. The predictions of the formulae agree with the experimental observations very well (Fig. 1a, 1b). The empirical formula of genome size is the start of our theory, which can be verified by many agreements between its predictions and experimental observations (especially the detailed agreements, Fig. 1, 3 and 4).

The formula of genome size for contemporary species can help us write down the formula of genome size evolution from $t = T_0 = 3,800$ million years ago (Ma) (the beginning of life [12]) to $t = 0$ (today). We introduced a function $s(t)$ to describe the overall trend of the genome size evolution according to the distribution of species in the $\eta - \theta$ plane. This is the

main assumption in our theory. We can distinguish two phases in genome size evolution (Fig. 2a). In phase *I*, all the species in the lower triangle of the $\eta - \theta$ plane are simple prokaryotes and their non-coding DNA contents are low. In phase *II*, all the species in the upper triangle of the $\eta - \theta$ plane are eukaryotes, and the non-coding DNA content increased to the maximum value η^* . It is reasonable, therefore, to take the critical event that divides the two phases as the Cambrian explosion.

Thus, we can obtain the formula of genome size evolution: $s_I(t) = s_1 \exp(t/\tau_1)$ for phase *I* and $s_{II}(t) = s_2 \exp(t/\tau_2)$ for phase *II*, where $s_1 = 1.98 \times 10^7$ bp, $\tau_1 = 644$ million years and $s_2 = 1.65 \times 10^9$ bp, $\tau_2 = 106$ million years (Fig. 2b). The result qualitatively agrees with the straightforward (but a little coarse) estimation of genome size evolution in Ref. [13] in that (i) both genome size evolution increase exponentially (namely linearly in Fig. 2b) and (ii) there is a unique turning point in genome size evolution for our result or for the estimate (Fig. 2b). As expected, the dividing value of genome size in our theory $s_I(T_c) = s_{II}(T_c) = s_0$ agrees with the maximum prokaryotic genome size in observation [8].

Explanation of the C-value enigma. The C-value enigma is apparently concerned with the lack of correlation between genome size and morphological complexity but profoundly with the nature of the Cambrian explosion. According to the genome size formula, we obtained some general properties of genome size evolution, hence major questions of the C-value enigma can be explained.

According to the genome size evolution formula, we can distinguish two speeds of genome size evolution. In phase *I*, the genome size doubled in about every 466 million years on the whole. And in phase *II*, the genome size doubled in about every 73 million years on the whole. So, the speed of genome size evolution for phase *II* (mainly non-coding DNA increasing) is much faster than that for phase *I* (mainly coding DNA increasing). The pattern of expo-

nential increment can be simply understood by the relation $\Delta s(t) \propto s \Delta t$ for the two phases respectively. The overall picture of the genome size evolution reflects the entire roadmap of the biological complexity evolution, which is helpful to understand the macroevolution.

The Cambrian explosion can help to account for the genome size ranges in taxa. All phyla appeared almost simultaneously in the Cambrian explosion. In the evolution, therefore, η increases from $\bar{\eta}$ to η^* for each phylum (Fig. 2a). The genome size in a phylum varies by about $\Delta = \lg \exp \frac{\eta^* - \bar{\eta}}{a} \sim 2.4$ orders of magnitude (Fig. 3). The history of a class is generally shorter than that of a phylum. So the genome size range in a class is less than that in a phylum, which varies by about $\delta = \lg \exp \frac{\Delta \theta}{b} \sim 0.5$ orders of magnitude (Fig. 3), where the uncertainty $\Delta \theta$ is estimated by 0.2 (Fig. 2a). Furthermore, we can explain the lack of correlation between genome size and morphological complexity. The origin of phyla in the Cambrian explosion related to the appearance of kernels of gene regulatory networks, whose complexity varied notably. But the C-values of species in different phyla did not vary notably [5]. So the discrepancy between genome size and eukaryotic complexity happened from scratch (Fig. 3).

Three clusters of prokaryotes C_{Gram-} , C_{Gram+} and C_{small} can be distinguished in the lower triangle of the $\eta - \theta$ plane (Fig. 2a), where Gram negative bacteria, Gram positive bacteria and bacteria with small genome size are in the majority respectively [14]. We evenly distributed 6038 dots (representing "species") in three symmetric areas enclosing C_{Gram-} , C_{Gram+} and C_{small} in Fig. 4a (the same areas with Fig. 2a). After projecting the three symmetric areas in plane by the non-linear transformation Eqn. 1, we obtained three asymmetric areas C'_{Gram-} , C'_{Gram+} and C'_{small} in $\eta - s$ plane in Fig. 4c. Finally, we obtained the prokaryotic genome size distribution in Fig. 4b by counting the numbers of species in each genome size section with identical width in Fig. 4c.

Timing of the Cambrian explosion. The time T_c for the Cambrian explosion can be calculated

according to the formula of genome size evolution. The function $s_I(t)$ represents the coding DNA evolution. Its extrapolated value $s_I(0) = s_1$ represents the size of coding DNA at present. And the value $s_{II}(0) = s_2$ represents the total genome size at present. For the coding DNA content at present, we obtained an equation between the experimental data and the theoretical prediction $1 - \eta^* = s_1/s_2$, where s_1 and s_2 are functions of T_c . According to this equation, we have

$$T_c = T_0(1 - (\frac{b}{1 - \bar{\eta}} \ln(1 - \eta^*) + \frac{b}{a} \frac{\eta^* - \bar{\eta}}{1 - \bar{\eta}} + 1)^{-1}) \equiv f(\eta^*). \quad (2)$$

This is the formula to calculate the Cambrian explosion time by C-value clock, which radically differs from molecular clock estimates (Fig. 2c) [15] [16]. The value η^* should be of the species whose η is the largest and whose complexity is the greatest. The best choice is no other than human: $\eta^* = 0.988$ [17] [18]. Therefore, we obtained the Cambrian explosion time $T_c = f(0.988) = 560$ Ma. Our result agrees with the fossil records very well (Fig. 2d).

This main result of C-value clock shows that the Cambrian explosion corresponds to a turning point in genome size evolution. It is for the first time, to our knowledge, to successfully mediate timing of the Cambrian explosion between paleontology and molecular biology. Considering the sensitive relationship between T_c and η^* . (Fig. 2d), it is remarkable to calculate almost the exact time of the Cambrian explosion by the non-coding DNA content of human genome. The subtle relationship $T_c = f(\eta^*)$ indicates the close relationship between the rapid expansion of noncoding DNA and the cause of the Cambrian explosion. The genetic mechanism can give us a clear and in-depth understanding of the Cambrian explosion. Both development and evolution of the animal body plans should be studied at the level of gene regulatory networks [5] [19]. The appearance of genomic regulatory systems may be a prerequisite for the animal evolution. And the phylum-specific or subphylum-specific kernels of gene regulatory networks may explain the conservation of major phyletic characters ever since the Cambrian [19].

According to Eqn. 2, we obtained $\frac{\Delta T_c}{T_c} = -75 \frac{\Delta \eta^*}{\eta^*} + \frac{\Delta T_0}{T_0} - 5.2 \frac{\Delta a}{a} + 0.85 \frac{\Delta b}{b} - 0.57 \frac{\Delta \bar{\eta}}{\bar{\eta}}$. The error of T_c in prediction, therefore, mainly comes from the parameter η^* . If considering the uncertainty in human gene prediction, the error of coding DNA content in human genome is about 10% [17]. Hence we obtained that the value of T_c in prediction ranges from 502 Ma to 560 Ma. Even if the databases of complete genomes and proteomes may expand much in the future, the parameters in Eqn. 1 would change slightly. So our main results in this paper will still be valid. By the way, if choosing T_c as the date of the earliest known microfossils, i.e., $T_0 = 3,500$ Ma, the prediction would be $T_c = 516$ Ma. There is a notable discrepancy between the molecular clock estimates and the fossil records [16] [20] [21]. Obviously, the C-value clock works better than the molecular clocks for this problem. We can conclude that the C-value clock estimate agrees with the fossil records in principle (Fig. 2d).

If comparing the time of evolution of life as a day, why did not the complex life appear in the morning or in the afternoon but appear around half past eight in the evening? In terms of the overall picture of genome size evolution in Fig. 2b, we can explain why the simple life had actually predominated on the planet for the first 6/7 time in the evolution. It is due to that the evolutionary speed for non-coding DNA is much faster than that for coding DNA. The Cambrian explosion can not happen in the first half of the period in the evolution. The reason is that s_1 is always less than s_2 such that the turning point had to appear later than the time $T_0/2$. Furthermore, it can be illustrated that the Cambrian explosion must happen very late because s_1 is in fact much less than s_2 at present, namely, the slope for the evolution of non-coding DNA is much steeper than the slope for the evolution of coding DNA (Fig. 2b).

Nature of the Cambrian explosion. The formula of genome size evolution opens up an opportunity to investigate the entire roadmap of evolution based on biological complexity. It is observed that the biological complexity increases faster and faster but not smoothly [22] [23]

[24]. The pattern that mass extinctions followed by rapid evolutionary radiations is widely considered to have fundamentally shaped the history of life. But it is not the answer to the case of the Cambrian explosion. The evolution is not only a mixture of accidental events. The one with less perseverance can never spend billions of years to assemble a jaguar by quarks! An overall mechanism of the evolution is required to explain the Cambrian explosion. The genome size evolution is just a problem on macroevolution. In our theory, the function $s(t)$ represents not only the trend of the genome size evolution but also the trend of the biological complexity evolution because the prokaryotic complexity is related to the genome size and the eukaryotic complexity is related to the non-coding DNA content [18]. The turning point in genome size evolution implies that there was a critical value of biological complexity in evolution, which is supported by the fact that both the genome size and the complexity of prokaryotes have never reached the size and complexity of eukaryotes. The constraint of the prokaryotic complexity demands a leap in biological complexity. As a result, the complex organisms successfully bypassed this constraint during Cambrian.

Several attempts have been proposed to explain the maximum prokaryotic complexity [25] [26] [8]. Its existence can be explained by the theory of accelerating networks [27]. It is suggested that prokaryotic complexity may have been limited throughout evolution by regulatory overhead, and conversely that complex eukaryotes must have bypassed this constraint by novel strategies [25] [22]. We give another explanation based on Kauffman's theory and the holographic principle [9] [11] [28]. The theory of self-organization provides deep insight into the spontaneous emergence of order which graces the living world [9]. The prokaryotic complexity should be understood as a dynamical system at the level of gene networks. So we can define prokaryotic complexity by information stored in Boolean networks, which is so immense that it can reach the maximum information content I_{univ} in the observed universe. Holographic bound in physics imposes a strict limit on the biological complexity. The information bridges between

biology and physics [29] [30]. We believe that the maximum prokaryotic complexity is constrained by the upper limit of information storage capacity in our universe. Hence the maximum complexity of accelerating networks in the above explanation can be given concretely.

The Cambrian explosion of animal phyla radically differs from all the other radiations such as the radiations of modern birds and mammals in the early Tertiary, because it corresponds to the unique critical event in the genome size evolution. The intrinsic reason of genome evolution determined the Cambrian explosion, during which the biological complexity leapt not only at the anatomical level but also at the molecular level. The stability of the genomic system became low before the Cambrian explosion because the old mechanism of evolution was suffocated. At this critical moment, any extrinsic factors were qualified to turn the evolution to a new direction. Numerous complex animal body plans were destined to come at a certain time. In contrast, the causes of other radiations were full of uncertainty. The nature of the Cambrian explosion must be studied in a broader context than before. The Cambrian explosion and the origin of life were the most important events in the evolution from nonliving systems to living systems. We believe that the C-value enigma and the Cambrian explosion will help us uncover the intricate mechanism in evolution. A multidisciplinary framework has been established in our work to explain the Cambrian explosion (see Supplementary Figure 1), which will shed light on the essence of evolution.

METHODS

The definition of correlation polar angle θ and its biological meaning. The correlation polar angle indicates the evolutionary relationship, whose role in the C-value clock is as important as the role of sequence similarities in molecular clocks. The correlation polar angle can be defined

according to protein length distributions, which helped in discovery of the formula of genome size when we fortunately realized the relationship between genome size S and the correlation polar angle θ . In the followings, we define the correlation polar angle firstly. Then we explain its biological meaning.

The protein length distribution is an intrinsic property of a species, which is defined as a distribution (namely a vector) $\mathbf{D} = (D_1, D_2, \dots, D_n, \dots)$: there are D_n proteins with length n in the complete proteome of the species. Our data of the protein length distributions are obtained from the data of 106 complete proteomes in the database Predictions for Entire Proteomes [32]. The normalized vector of protein length distribution \mathbf{d} is defined by the direction of vector \mathbf{D} :

$$\mathbf{d} \equiv \mathbf{D} / \sqrt{\mathbf{D} \cdot \mathbf{D}} = \mathbf{D} / \sqrt{\sum_n D_n^2}.$$

Because there are few proteins longer than 3000 amino acids in a complete proteome (Supplementary Figure 2c), we can neglect them and set the length 3000 as the cutoff of protein length in the calculation. Hence both \mathbf{D} and \mathbf{d} are 3000-dimensional vectors. Thus each species corresponds to a point on the 3000-dimensional unit sphere (Supplementary Figure 4a). The polar axis of the spherical coordinates (Supplementary Figure 4a) can be defined by the direction of the vector of the total protein length distribution of the 106 species (Supplementary Figure 2c)

$$\mathbf{Z} = \sum_{i \in 106 \text{ species}} \mathbf{D}(i).$$

And we denote the normalized vector of \mathbf{Z} as the unit vector \mathbf{z} of polar axis, the corresponding point of which situates at the center of the swarm of 106 points on the unit sphere (Supplementary Figure 4a). The correlation polar angle θ of a species is defined by the polar angle of the corresponding vector of protein length distribution:

$$\theta \equiv \frac{2}{\pi} \arccos(\mathbf{d} \cdot \mathbf{z}),$$

where the factor $\frac{2}{\pi}$ is added in order that the value of θ ranges from 0 to 1.

The biological meaning of the correlation polar angle can be interpreted as the average evolutionary relationship between an species and all the other species (Supplementary Figure 3b). The less the value of θ is, the closer the average evolutionary relationship is. This interpretation is based on the following two considerations: (1) Let vectors $\mathbf{d}(i)$ and $\mathbf{d}(j)$ correspond the protein length distributions of two species i and j (Supplementary Figure 4a). The correlation between the two protein length distributions can be defined by their inner product $C_{ij} = \mathbf{d}(i) \cdot \mathbf{d}(j)$. Hence we obtain the correlation matrix (C_{ij}) (Supplementary Figure 3a). We can see that the evolutionary relationship is closely related to the correlation between the protein length distributions. The correlation polar angle θ for species i can be interpreted as the average evolutionary relationship according to (compare Supplementary Figure 3a and 3b):

$$\begin{aligned} \cos\left(\frac{\pi}{2}\theta\right) &= \sum_{j \in 106 \text{ species}} \mathbf{d}(i) \cdot \mathbf{D}(j) / \sqrt{\mathbf{Z} \cdot \mathbf{Z}} \\ &= \sum_{j \in 106 \text{ species}} \cos\left(\frac{\pi}{2}\theta_{ij}\right) w(j), \end{aligned}$$

where $\theta_{ij} = \frac{2}{\pi} \arccos(C_{ij})$ is the correlation angle between two species and $w(j) = \sqrt{\mathbf{D}(j) \cdot \mathbf{D}(j)} / \sqrt{\mathbf{Z} \cdot \mathbf{Z}}$ is the weight for species j in the summation. (2) An auxiliary polar axis \mathbf{z}' can be defined by another direction differed from the polar axis. For example, we chose the direction corresponds to the distribution in Supplementary Figure 2d, hence the auxiliary polar angle is defined by $\phi \equiv \frac{2}{\pi} \arccos(\mathbf{d} \cdot \mathbf{z}')$ (Supplementary Figure 4a). Then the high dimensional unit sphere (dim=3000) can be projected to a two dimensional $\theta - \phi$ plane, where eukaryotes, archaeobacteria and eubacteria gather together in three areas respectively (Supplementary Figure 4b) and the closely related species also form clusters in the $\theta - \phi$ plane. So the correlation polar angle is a useful tool to study the evolutionary relationship. The conclusion is still valid if we choose other directions as the auxiliary polar angle.

Derivation of Eqn. 1: the genome size $S(\eta, \theta)$. We found that $\ln S$ decreases linearly with

θ (Supplementary Figure 5a) but increases linearly with η (Supplementary Figure 5b) on the whole. Hence, we wrote down the relation:

$$\ln S = \ln s_0 + \frac{\eta}{a} - \frac{\theta}{b}.$$

According to the biological data of genome size, η and θ (Supplementary Table 2), we obtained the empirical formula of genome size Eqn. 1 and its coefficients a , b and s_0 by least squares. Similarly, we obtained the gene number formula

$$N(\eta, \theta) = n_0 \exp\left(\frac{\eta}{a'} - \frac{\theta}{b'}\right).$$

The value of η varies little for prokaryotes in both formulae and $b \approx b'$, so the genome size is approximately proportional to the gene numbers:

$$\frac{S}{N} \approx \frac{s_0}{n_0} \exp\left(\bar{\eta}\left(\frac{1}{a} - \frac{1}{a'}\right)\right) = 842,$$

which is near to the ratio in observation [8]. But such linear relationship is destroyed for eukaryotes because of the vast variation of η .

The relationship between non-coding DNA N_{nc} and coding DNA N_c for eukaryotes. The average protein length for eukaryotes is about 450 amino acids, so the logarithm of coding DNA for eukaryotes is about $\log N_c = \log(3 \times 450 n_0) + \frac{\eta}{a'} - \frac{\bar{\eta}}{b'}$ according to the gene number formula. And the logarithm of non-coding DNA is about $\log N_{nc} = \log s_0 + \frac{\eta}{a} - \frac{\bar{\eta}}{b} + \log \eta$ according to the genome size formula. So we have

$$\begin{aligned} \log N_{nc} &= \frac{a'}{a} \log N_c + \log s_0 - \frac{a'}{a} \log(1350 n_0) - \frac{\bar{\eta}}{b} + \frac{\bar{\eta}}{b'} \frac{a'}{a} + \log \eta \\ &\approx 2.81 \log N_c - 12.5, \end{aligned}$$

where we let $\log \eta \approx \log 0.5$ in calculation. According to the experimental observation (Figure 1 in Ref. [33]), we obtain the relationship $\log N_{nc} = 2.82 \log N_c - 12.8$ between non-coding

DNA and coding DNA for actual species on the whole if choosing two points (6.8, 6.4) and (7.9, 9.5) in Figure 1 in Ref. [33] to determine the linear relationship. Our result agrees with the experimental observation perfectly.

The genome size evolution function $s(t)$. We can observe a right-angled distribution of the contemporary species in the $\eta - \theta$ plane (Fig. 2a). The prokaryotes and the eukaryotes are separated by the diagonal line $\eta = \theta$. An underlying mechanism of genome size evolution is necessary to account for the distribution. Some species originated earlier while the other originated later. As a result, the distribution of species in the $\eta - \theta$ plane has recorded the information of genome size evolution. Hence we can write down the genome size evolution function.

The prokaryotes situate around the horizontal line $\eta = \bar{\eta} = 0.115$, where $\bar{\eta}$ is the average of η for 48 prokaryotes (see Supplementary Table 1 and 2). According to Eqn. 1, the trend of the genome size evolution for prokaryotes increases when θ decreases. When θ is close to 1, there is few species because the genome size is too small as for the contemporary species. On the other hand, the eukaryotes situate around the vertical line $\theta = \bar{\eta}$ and the trend of their genome size evolution increases when η increases.

We introduced a function $s(t)$ to describe the overall trend of the genome size evolution according to the right-angled distribution in observation, whose turning point corresponds to the largest genome size of prokaryotes (Fig 2a). It is reasonable to define that the genome size evolution function $s(t)$ evolves leftwards along the horizontal line $\eta = \bar{\eta}$ and consequently upwards along the vertical line $\theta = \bar{\eta}$ in the $\eta - \theta$ plane. This definition of genome size evolution function agrees not only with the right-angled distribution of species in the $\eta - \theta$ plane but also with the trend of the genome size evolution from small to large on the whole.

Derivation of Eqn. 2: the Cambrian explosion time T_c . In phase I, $\eta(t) = \bar{\eta}$, and $\theta(t)$ decreases linearly from 1 to $\bar{\eta}$, i.e., $\theta(t) = 1 - \frac{(1-\bar{\eta})(t-T_0)}{T_c-T_0}$. So we have

$$s_I(t) \equiv s_0 \exp\left(\frac{\eta(t)}{a} - \frac{\theta(t)}{b}\right) = s_1 \exp(t/\tau_1),$$

where $s_1 = s_0 \exp(\frac{\bar{\eta}}{a} - \frac{T_c - \bar{\eta}T_0}{b(T_c - T_0)})$ and $\tau_1 = \frac{b(T_c - T_0)}{1 - \bar{\eta}}$. Incidentally, we have $s' \equiv s_I(T_0) = s_0 \exp(\frac{\bar{\eta}}{a} - \frac{1}{b})$. And in phase II, $\theta(t) = \bar{\eta}$ and $\eta(t) = \eta^* - (\eta^* - \bar{\eta})t/T_c$. So we have

$$s_{II}(t) \equiv s_0 \exp\left(\frac{\eta(t)}{a} - \frac{\theta(t)}{b}\right) = s_2 \exp(t/\tau_2),$$

where $s_2 = s_0 \exp(\frac{\eta^*}{a} - \frac{\bar{\eta}}{b})$ and $\tau_2 = \frac{a(-T_c)}{\eta^* - \bar{\eta}}$. Finally, substituting the expressions of s_1 and s_2 into the equation $1 - \eta^* = s_1/s_2$, we obtained Eqn. 2.

Upper limit of the prokaryotic complexity. Boolean networks have for several decades received much attention in understanding the underlying mechanism in evo-devo biology [9] [34]. We define the network N_L as a Boolean network whose nodes are all possible protein sequences with the length less than L . The size of state space of N_L is $\sim 2^{20^L}$ in that N_L has about 20^L nodes. According to Shannon's theory, the information stored in this network is $I_{net} \sim \log_2 2^{20^L} = 20^L$ bits (Supplementary Figure 6). Types of prokaryotes can be interpreted by attractors of the Boolean network N_L , which are robust against perturbations in evolution [34]. An actual genome of an organism can be denoted by one point amongst the total $\sim 2^{20^L}$ points in the state space of N_L . Based on the consideration that the biological complexity should be evaluated at the level of gene regulatory networks, the prokaryotic complexity can be defined by the information I_{net} stored in N_L . Its value is much greater than the information stored in the genetic sequences; the latter is not sufficient to measure the biological complexity for overlooking the complexity at the level of gene networks. This definition does not apply to eukaryotic complexity, which may involve RNA regulations [22].

We can show that the constrained maximum complexity of unicellular organisms can be explained by the upper limit of information stored in the finite space. There was a great achievement in the knowledge of fundamental laws in nature, which originated in the field of quantum gravity [35] [36] [28]. It claims that the information storage capacity of a spatially finite system must be limited by its boundary area measured in fourfold Planck area unless the second law of thermodynamics is untrue. Consequently, we can obtain the maximum information storage capacity in the observable universe as $I_{univ} \approx 10^{122}$ bits [37], which is a strict limit on the information content not only for physical systems but also for living organisms. Let $I_{net} \sim I_{univ}$, we obtained $L \sim 94$ amino acids, which dramatically corresponds to the most probable protein length for prokaryotes (Supplementary Figure 2b) [38]. So the information stored in the prokaryotic gene networks is so large as to be comparable to I_{univ} . Thus we have demonstrated the equivalence between the prokaryotic complexity and the information content I_{univ} in our universe. We might say that what kind of spacetime determines what kind of life. A certain vast spacetime is necessary to accommodate the immense information stored in life.

We are grateful to Hefeng Wang, Lei Zhang, and Yachao Liu for valuable discussions. Supported by NSF of China Grant No. of 10374075.

References

- [1] Valentine, J. W., Erwin, D. H. & Jablonski, D. Developmental evolution of metazoan body plans: the fossil evidence. *Dev. Biol.* **173**, 373-381 (1996).
- [2] Knoll, A. H. & Carroll, S. B. Early animal evolution: emerging views from comparative biology and geology. *Science* **284**, 2129-2137 (1999).
- [3] Conway Morris, S. The Cambrian explosion: Slow-fuse or megatonnage? *Proc. Natl. Acad. Sci. USA* **97**, 4426-4429 (2000).

- [4] Shu, D.-G. et al. Primitive deuterostomes from the Chengjiang Lagerstätte (Lower Cambrian, China). *Nature* **414**, 419-424 (2001).
- [5] Davidson, E. H. & Erwin, D. H. Gene regulatory networks and the evolution of animal body plans. *Science* **311**, 796-800 (2006).
- [6] Larroux, C. The NK Homeobox Gene Cluster Predates the Origin of Hox Genes. *Current Biology* **17**, 706-710 (2007).
- [7] Peltier, W. R., Liu, Y. & Crowley, J. W. Snowball Earth prevention by dissolved organic carbon remineralization. *Nature* **450**, 813-818 (2007).
- [8] Gregory T. R. ed. *The evolution of the genome* (Elsevier, Amsterdam, 2005).
- [9] Kauffman, S. A. *The origins of order* (Oxford Univ. Press, New York, 1993).
- [10] Solé, R. V., Fernández, P. & Kauffman, S. A. Adaptive walks in a gene network model of morphogenesis: insights into the Cambrian explosion. *arXiv Preprint Archive* [online], <http://arXiv.org/abstract/q-bio/0311013v1> (2003).
- [11] Bekenstein, J. D. Information in the holographic universe. *Sci. Am.* **289**, 58-65 (2003).
- [12] Mojzsis, S. J. et al. Evidence for life on Earth before 3,800 million years ago. *Nature* **384**, 55-59 (1996).
- [13] Sharov, A. A. Genome increase as a clock for the origin and evolution of life. *Biology Direct* **1**:17 (2007).
- [14] Trevors, J. T. Genome size in bacteria. *Antonie van Leeuwenhoek* **69**, 293-303 (1996).
- [15] Peterson, K. J. et al. Estimating metazoan divergence times with a molecular clock. *Proc. Natl. Acad. Sci. USA* **101**, 6536-6541 (2004).

- [16] Kumar, S. Molecular clocks: four decades of evolution. *Nat. Rev. Genet.* **6**, 654-662 (2005).
- [17] International Human Genome Sequencing Consortium, Finishing the euchromatic sequence of the human genome. *Nature* **431**, 931-945 (2004).
- [18] Taft, R. J. & Mattick, J. S. Increasing biological complexity is positively correlated with the relative genome-wide expansion of non-protein-coding DNA sequences. *arXiv Preprint Archive* [online], <http://www.arxiv.org/abs/q-bio.GN/0401020> (2004).
- [19] Davidson, E. H. *The regulatory genome: gene regulatory networks in development and evolution* (Elsevier, Amsterdam, 2006).
- [20] Hedges, S. B. & Kumar, S. Genomic clocks and evolutionary timescales. *Trends Genet.* **19**, 200-206 (2003).
- [21] Bromham, L., Penny, D. The modern molecular clocks. *Nat. Rev. Genet.* **4**, 216-224 (2003).
- [22] Mattick, J. S. RNA regulation: a new genetics? *Nature Rev. Genet.* **5**, 316-323 (2004).
- [23] Knoll, A. H. Proterozoic and early Cambrian protists: evidence for accelerating evolutionary tempo. *Proc. Natl. Acad. Sci. USA* **91**, 6743-6750 (1994).
- [24] Adami, C., Ofria, C. & Collier, T. C. Evolution of biological complexity. *Proc. Natl. Acad. Sci. USA* **97**, 4463-4468 (2000).
- [25] Croft, L. J., Lercher, M. J., Gagen, M. J. & Mattick, J. S. Is prokaryotic complexity limited by accelerated growth in regulatory overhead. *arXiv Preprint Archive* [online], <http://arxiv.org/abs/q-bio.MN/0311021> (2003).

- [26] Lynch, M. & Conery, J. S. The origins of genome complexity. *Science* **302**, 1401-1404 (2003).
- [27] Mattick, J. S. & Gagen, M. J. Accelerating Networks. *Science* **307**, 856-857 (2005).
- [28] Bousso, R. The holographic principle. *Rev. Mod. Phys.* **74**, 825-874 (2002).
- [29] Wada, A. Bioinformatics - the necessity of the quest for ‘first principles’ in life. *Bioinformatics* **16**, 663-664 (2000).
- [30] Wheeler, J. A. Information, physics, quantum: the search for the links, in *Proceedings of 3rd international symposium foundations of quantum mechanics*, pp. 354-368 (Tokyo, 1989).
- [31] Gregory T. R. Macroevolution, hierarchy theory, and the C-value enigma. *Paleobiology* **30**, 179-202 (2004).
- [32] Carter, P., Liu, J. & Rost, B. PEP: Predictions for Entire Proteomes. *Nucleic Acids Research* **31**, 410-413 (2003). The URL of the database PEP is <http://cubic.bioc.columbia.edu/pep>.
- [33] Ahnert, S. E., Fink, T. M. A. & Zinovyev, A. How much non-coding DNA do eukaryotes require? *arXiv Preprint Archive* [online], <http://www.arxiv.org/abs/q-bio.GN/0611047v4> (2008).
- [34] Shmulevich, I, Kauffman, S. A. & Aldana, M. Eukaryotic cells are dynamically ordered or critical but not chaotic. *Proc. Natl. Acad. Sci. USA* **102**, 13439-13444 (2005).
- [35] Bekenstein, J. D. Black holes and the second law. *Lett. Nuovo. Cim.* **4**, 737-740 (1972).
- [36] Hawking, S. W. Black hole explosions? *Nature* **248**, 30-31 (1974).

- [37] Susskind, L. & Lindesay, J. *An introduction to black holes, information, and the string theory revolution* (World Scientific, Singapore, 2005).
- [38] Rost, B. Did evolution leap to create the protein universe? *Curr. Opin. Stru. Biol.* **12**, 409-416 (2002).

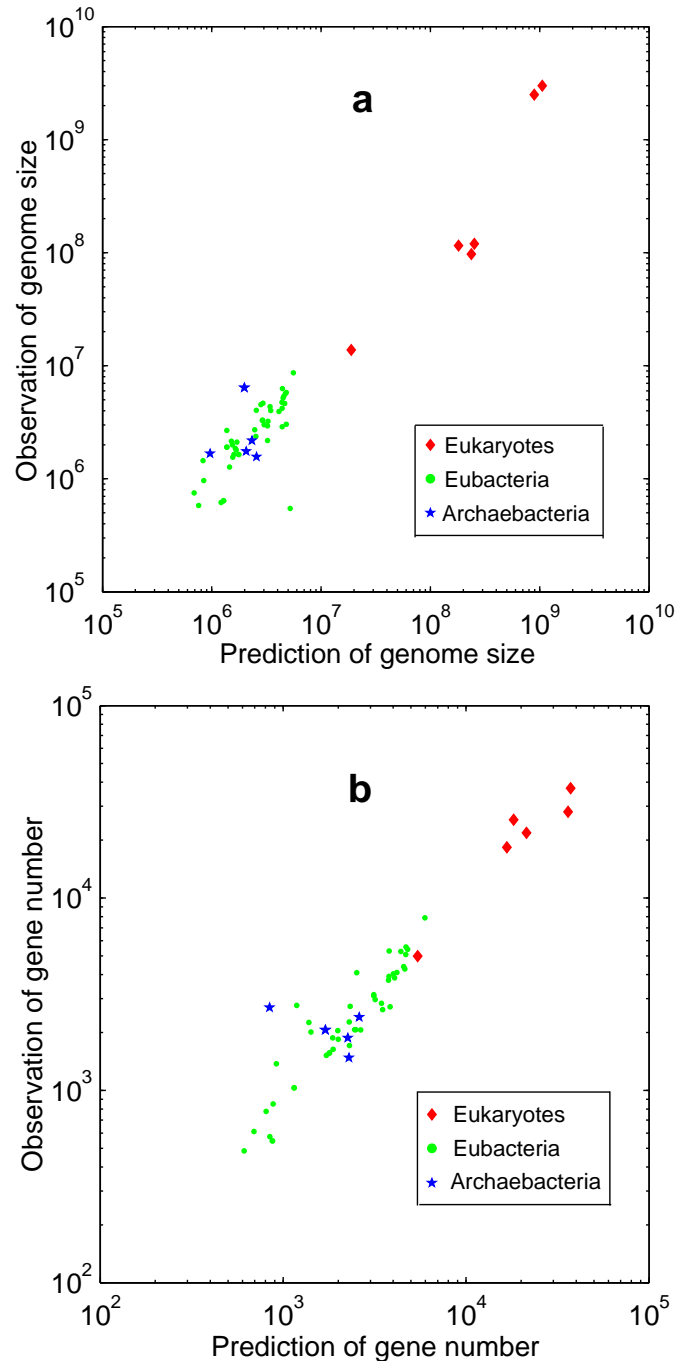


Figure 1: **Comparison between predictions and observations for genome size and gene number.** Our results quite fit the experimental observations not only for prokaryotes but also for eukaryotes. **a**, Genome size (correlation coefficient $r = 0.974$). **b**, Gene number (correlation coefficient $r = 0.976$).

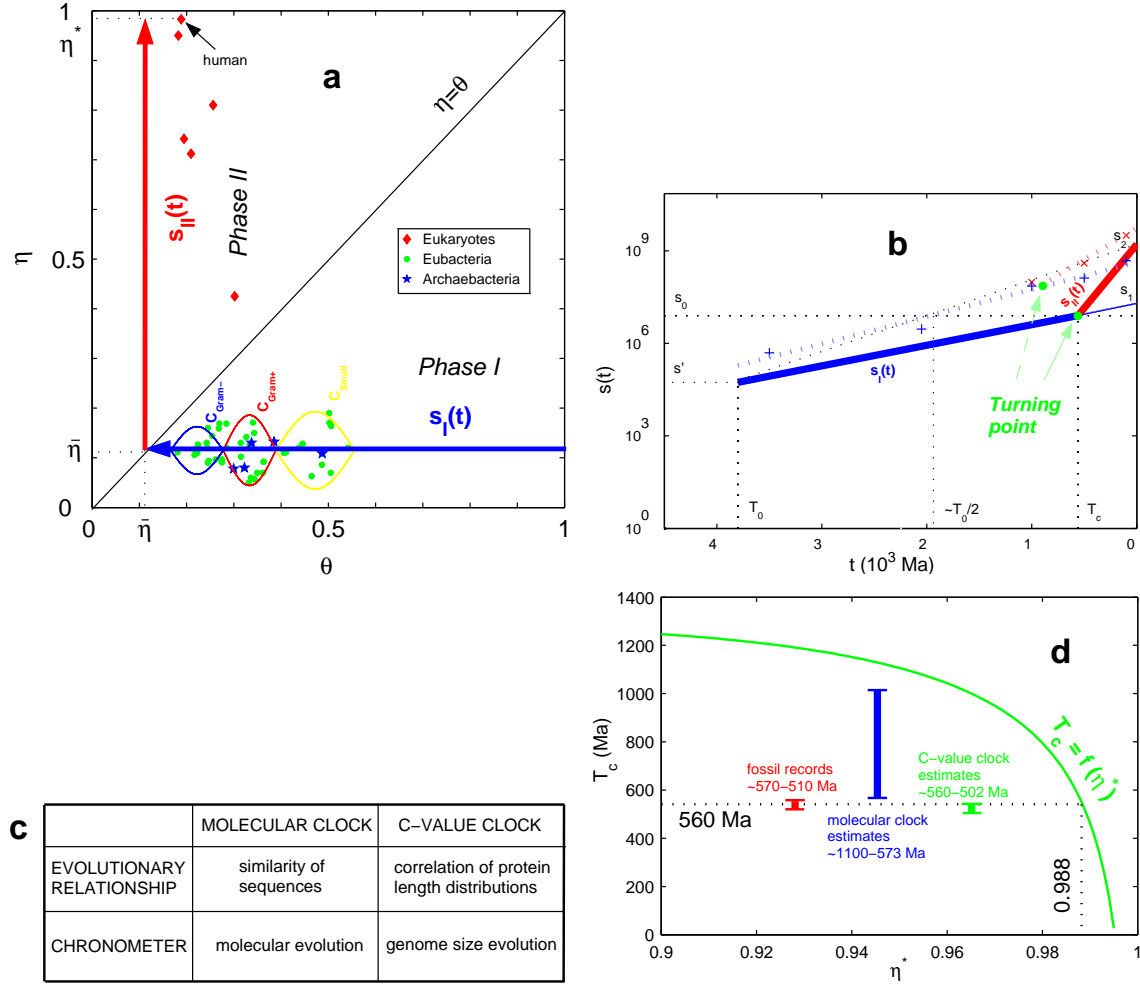


Figure 2: **Genome size evolution and the nature and timing of the Cambrian explosion.** **a**, The distribution of species in $\theta - \eta$ plane and the function of genome size evolution. **b**, The turning point of genome size evolution (red: total genetic DNA and blue: coding DNA). Our result (solid lines) is supported by the coarse estimate (thick dotted lines, data for estimate time and genome size for 5 taxa are obtained from Ref [13])). **c**, Comparison between the molecular clock and the C-value clock. **d**, A sensitive relationship $T_0 = f(\eta^*)$. If varying η^* a little, T_c will change much. The value of T_c ranges approximately from 502 Ma to 560 Ma according to the C-value clock estimate. The result by C-value clock agrees with the fossil records [3] better than the molecular clock estimates [16] [15]. There should be notable systematic errors in the usual method of molecular clock estimates.

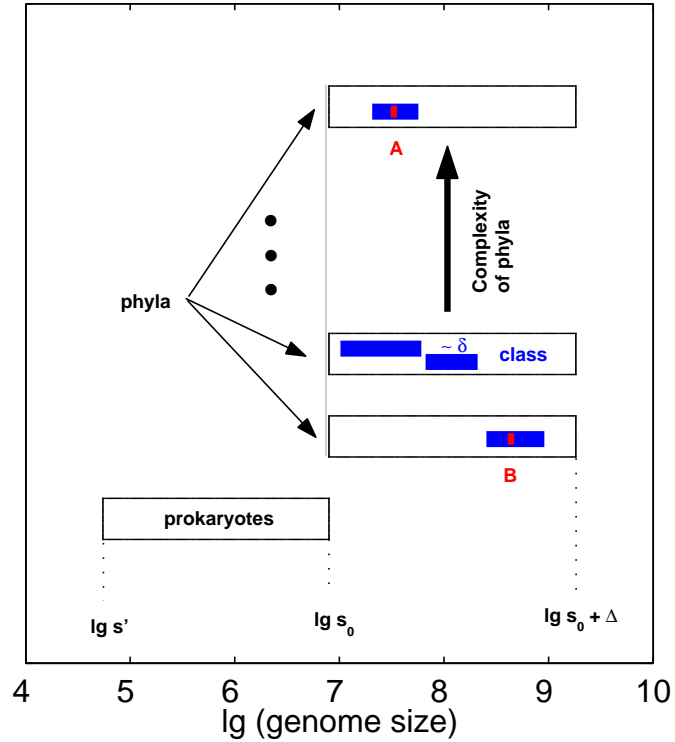


Figure 3: **Explanation of C-value enigma: genome size range and eukaryotic complexity.**

The ranges in genome size by order of magnitude ($\Delta \sim 2.4$ for phyla and $\delta \sim 0.5$ for classes) fit the experimental observations in general (see Fig. 1 in Ref. [31]). In observation, the genome sizes of majority phyla also vary by about 2 magnitudes and the genome sizes of majority classes vary by less than 1 magnitude [8]. The complexity of a species inherits from the complexity of the corresponding phylum in general, so the complexity of species *A* in a more complex phylum can potentially outstrip the complexity of species *B* in a less complex phylum, though the genome size of *A* is much less than that of *B*.

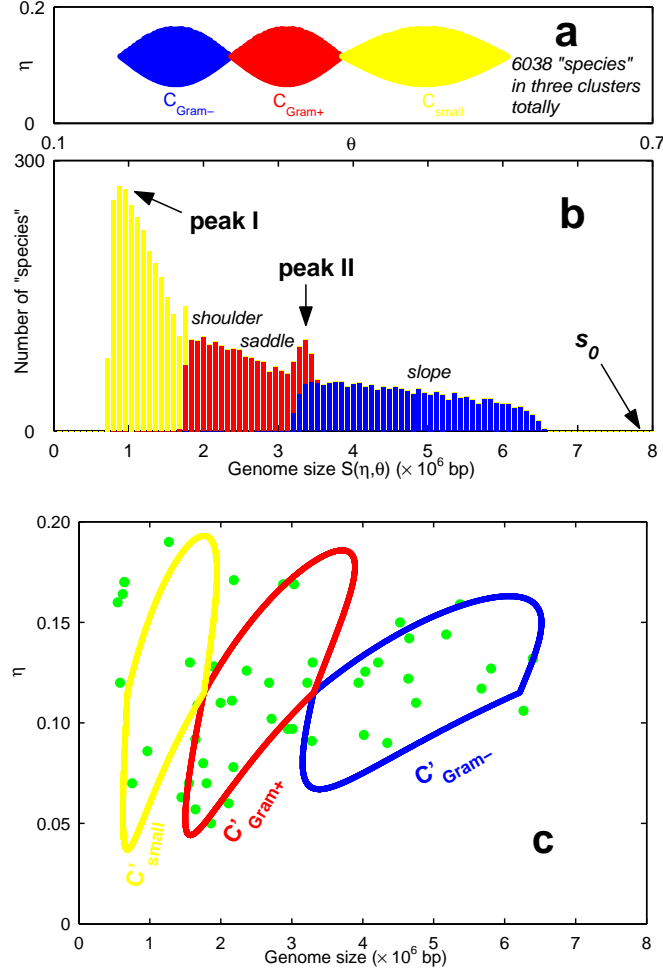


Figure 4: **Explanation of C-value enigma: prokaryotic genome size distribution.** **a**, Evenly distributed dots (representing "species") in three symmetric areas in $\theta - \eta$ plane. **b**, The prediction of prokaryotic genome size distribution quite fits the experimental observation. The principal characters of two peaks and their ratio in height and even the detailed characters such as shoulder, saddle and slope are almost the same in the actual genome size distribution in Fig. 10.12 in Ref. [8]. **c**, The prediction of prokaryotic distribution in $s - \eta$ plane (three asymmetric areas enclosing by lines) quite fits the intricate distribution of prokaryotes (green dots).

SUPPLEMENTARY INFORMATION

- Supplementary figures 1 ~ 6
- Supplementary tables 1 ~ 2

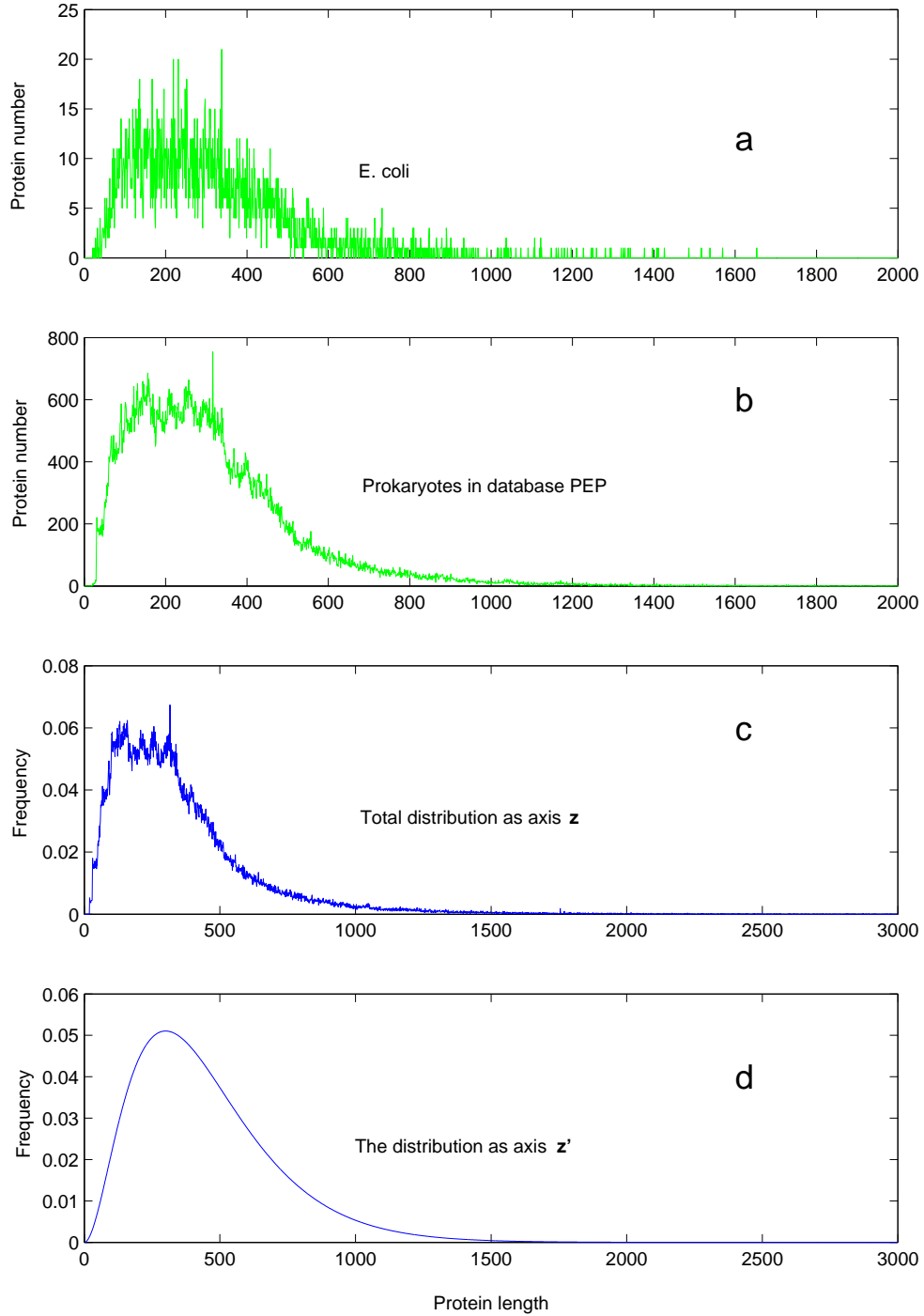


Figure 6: **Supplementary Figure 2: Protein length distributions.** **a**, An example of protein length distribution of *E. coli*. **b**, Total protein length distribution for prokaryotes. **c**, Total protein length distribution for all the species in database PEP, which can be taken as the polar axis z in the Supplementary Figure 4a. **d**, An outline of the protein length distribution, which can be taken as the polar axis z' in the Supplementary Figure 4a.

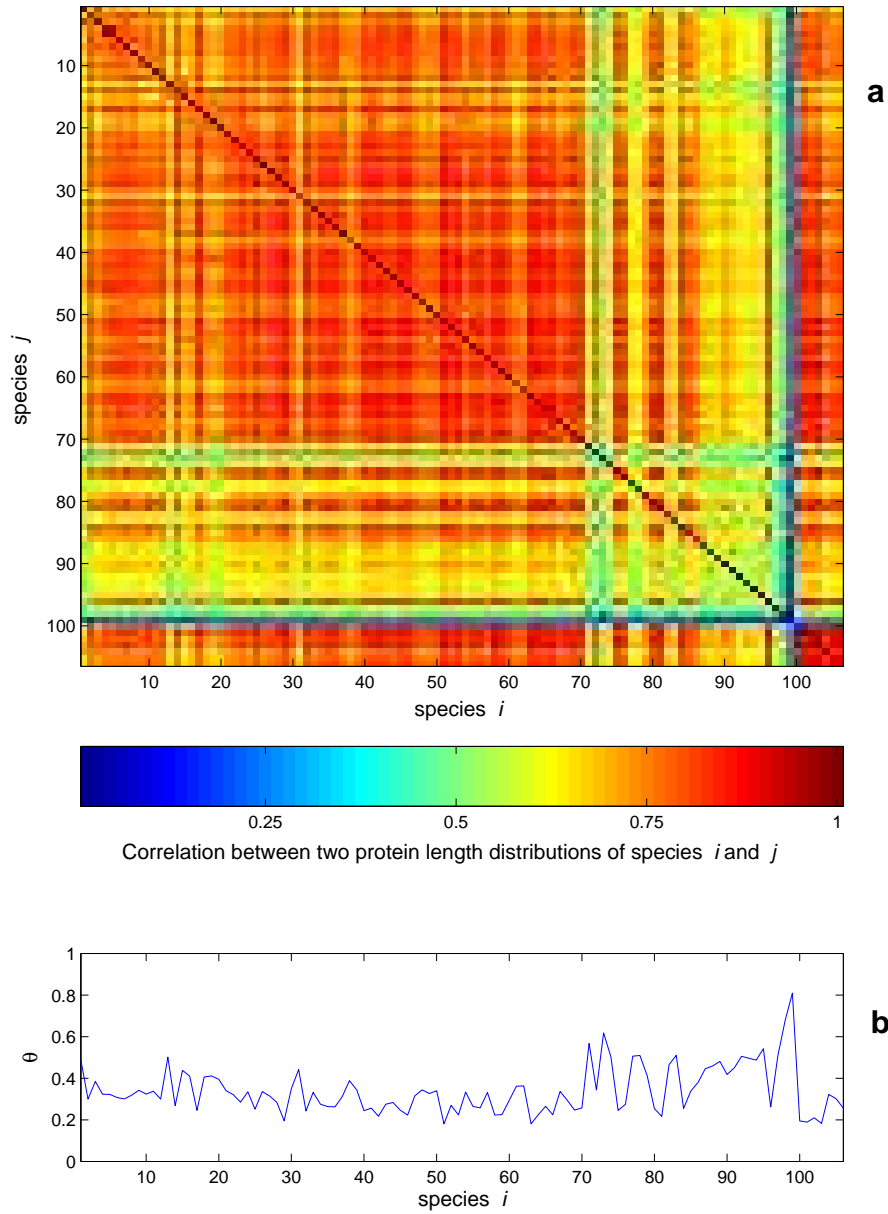


Figure 7: Supplementary Figure 3: The evolutionary relationship can be revealed by the correlation between protein length distributions. **a**, The correlation matrix (C_{ij}) represent the evolutionary relationship between any pairs of species i and j among the 106 species. The species in the matrix are ordered by the average protein length from short to long for archaeobacteria, eubacteria, virus and eukaryotes respectively. The species can be given concretely by the serial number in Supplementary Table 1 from the 1st position to the 106th position in the correlation matrix: 3, 8, 84, 65, 66, 83, 95, 51, 64, 82, 96, 63, 87, 9, 104, 49, 10, 40, 31, 93, 76, 91, 45, 94, 78, 57, 21, 90, 86, 53, 89, 11, 59, 61, 58, 62, 42, 13, 50, 34, 101, 4, 41, 60, 48, 33, 47, 26, 106, 56, 20, 35, 5, 100, 39, 2, 97, 46, 44, 37, 6, 54, 92, 85, 16, 81, 102, 38, 28, 15, 73, 77, 19, 23, 70, 18, 22, 24, 14, 69, 80, 17, 27, 103, 36, 79, 98, 30, 74, 29, 32, 99, 1, 75, 72, 12, 71, 52, 68, 25, 55, 7, 67, 105, 88, 43. **b**, The correlation polar angle θ for each of the 106 species (see Supplementary Table 2) can be interpreted as the average evolutionary relationship: the more the average correlation between protein length distributions is, the less the value of θ is; and the less the value of θ is, the closer the average evolutionary relationship is.

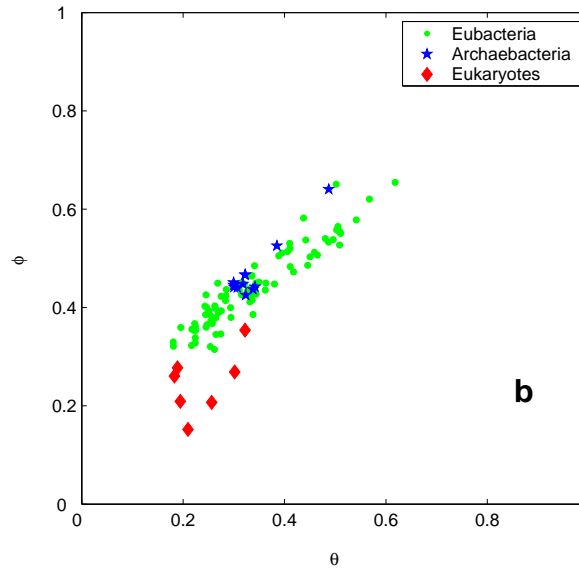
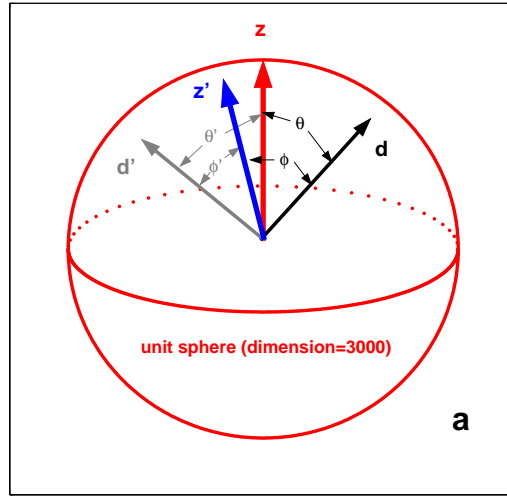


Figure 8: **Supplementary Figure 4: The correlation polar angle and the evolutionary relationship.** **a**, The correlation polar angle θ and the auxiliary angle ϕ . **b**, Distribution of three domains in the $\theta - \eta$ plane. The evolutionary relationship can be reflected by the correlation between the protein length distributions. Species in different domains gather together in different areas respectively.

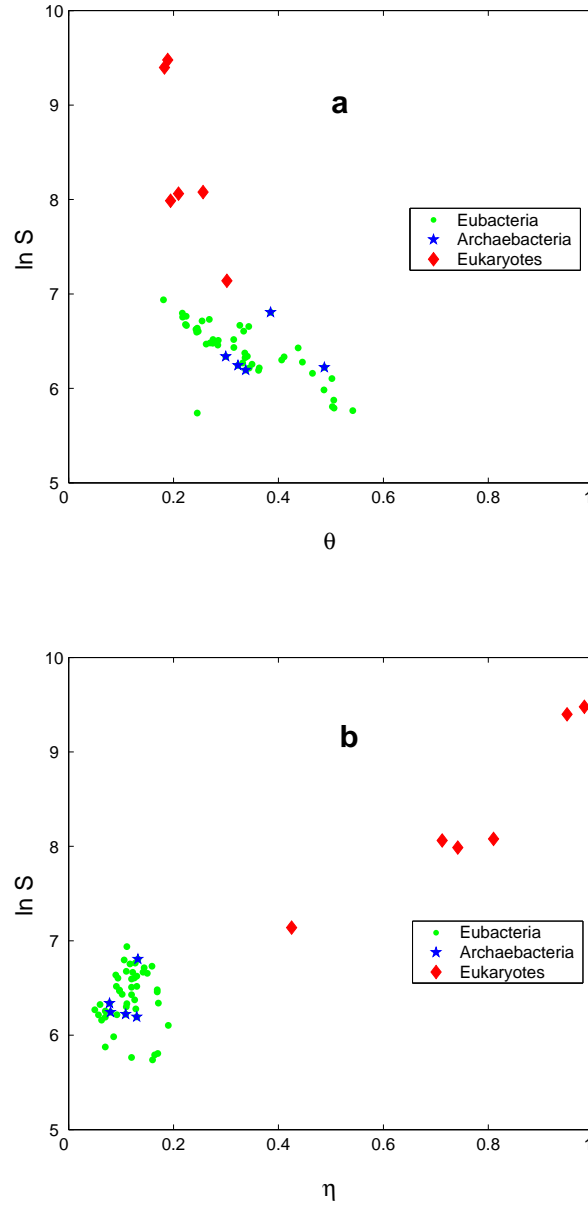


Figure 9: **Supplementary Figure 5: Relationship between the genome size and the non-coding DNA content and the correlation polar angle. a,** $\ln S$ increases when θ decreases on the whole. **b,** $\ln S$ increases when η increases on the whole.

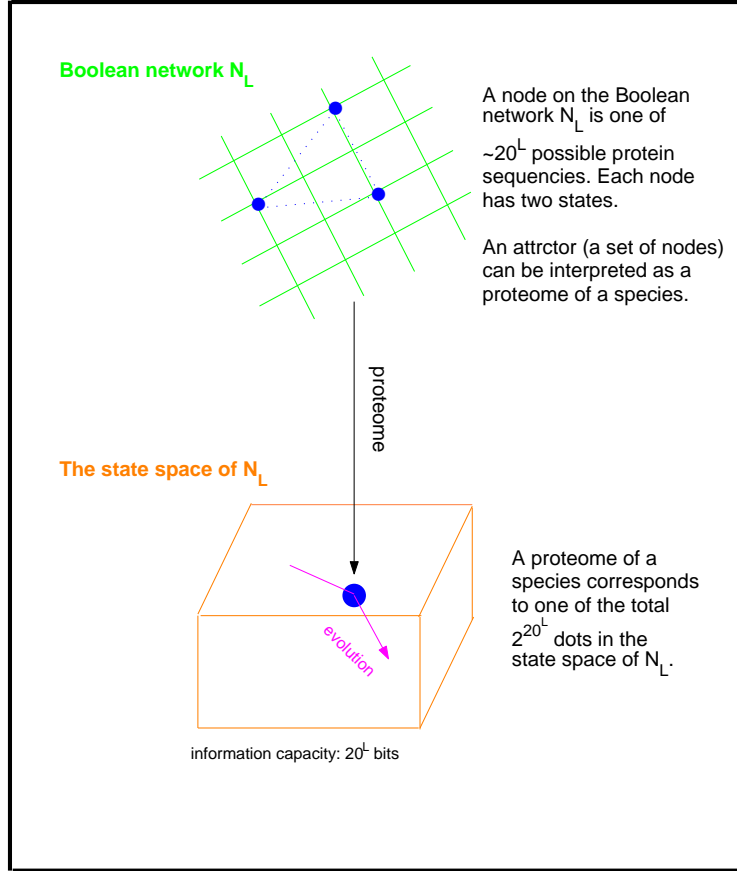


Figure 10: Supplementary Figure 6: Explanation of prokaryotic complexity by the Boolean network N_L and its state space. Each node on the network N_L is one of $\sim 20^L$ possible amino acid sequences, which has two states "on" or "off" according to the theory of Boolean networks. Each point in the state space of N_L represents a "proteome" (a set of "proteins" as an attractor of the Boolean network N_L whose states are "on"). The attractor is robust against the perturbations in evolution. The evolution of a species can be described by a trajectory of the evolving proteome of the species in the state space of N_L . An underlying evolutionary mechanism is necessary to determine the movement of the species in the global state space of N_L , so the complexity of the life system is proportional to the number of points in the state space of N_L . The information stored in gene networks (20^L bits) reflects the complexity of the life system, which is compatible to the maximum information stored in the observed universe I_{univ} .

Supplementary Table 1: Organisms in the database Predictions for Entire Proteomes PEP

Notes: There are 7 eukaryotes, 12 archaeobacteria, 85 eubacteria and 2 viruses in PEP.

(No. 1) PEP FILE: achfl.pep ORGANISM: Acholeplasma florum (Mesoplasma florum); A (M) florum; achfl DOMAIN: Eubacteria
(No. 2) PEP FILE: aciad.pep ORGANISM: Acinetobacter sp (strain ADP1); A sp ADP1; aciad DOMAIN: Eubacteria
(No. 3) PEP FILE: aerpe.pep ORGANISM: Aeropyrum pernix K1; A pernix K1; aerpe DOMAIN: Archaeobacteria
(No. 4) PEP FILE: agrt5.pep ORGANISM: Agrobacterium tumefaciens (strain C58 / ATCC 33970); A tumefaciens; agrt5 DOMAIN: Eubacteria
(No. 5) PEP FILE: agrtu.pep ORGANISM: Agrobacterium tumefaciens; A tumefaciens; agrtu DOMAIN: Eubacteria
(No. 6) PEP FILE: aquae.pep ORGANISM: Aquifex aeolicus; A aeolicus; aquae DOMAIN: Eubacteria
(No. 7) PEP FILE: arath.pep ORGANISM: Arabidopsis thaliana; A thaliana; arath DOMAIN: Eukaryote
(No. 8) PEP FILE: arcfu.pep ORGANISM: Achaeoglobus fulgidus; A fulgidus; arcfu DOMAIN: Archaeobacteria
(No. 9) PEP FILE: bacaa.pep ORGANISM: Bacillus anthracis (strain Ames); B anthracis_Ames; bacaa DOMAIN: Eubacteria
(No. 10) PEP FILE: bacce.pep ORGANISM: Bacillus cereus (ATCC 14579); B cereus (ATCC 14579); bacce DOMAIN: Eubacteria

(No. 11) PEP FILE: bacsu.pep ORGANISM: <i>Bacillus subtilis</i> ; B subtilis; bacsu DOMAIN: Eubacteria
(No. 12) PEP FILE: bactn.pep ORGANISM: <i>Bacteroides thetaiotaomicron</i> VPI-5482; B thetaiotaomicron VPI-5482; bactn DOMAIN: Eubacteria
(No. 13) PEP FILE: barhe.pep ORGANISM: <i>Bartonella henselae</i> (Houston-1); B henselae Houston-1; barhe DOMAIN: Eubacteria
(No. 14) PEP FILE: barqu.pep ORGANISM: <i>Bartonella quintana</i> (Toulouse); B quintana Toulouse; barqu DOMAIN: Eubacteria
(No. 15) PEP FILE: bdeba.pep ORGANISM: <i>Bdellovibrio bacteriovorus</i> ; B bacteriovorus; bdeba DOMAIN: Eubacteria
(No. 16) PEP FILE: borbr.pep ORGANISM: <i>Bordetella bronchiseptica</i> RB50; B bronchiseptica RB50; borbr DOMAIN: Eubacteria
(No. 17) PEP FILE: borbu.pep ORGANISM: <i>Borrelia burgdorferi</i> ; B burgdorferi; borbu DOMAIN: Eubacteria
(No. 18) PEP FILE: borpa.pep ORGANISM: <i>Bordetella parapertussis</i> ; B parapertussis; borpa DOMAIN: Eubacteria
(No. 19) PEP FILE: borpe.pep ORGANISM: <i>Bordetella pertussis</i> ; B pertussis; borpe DOMAIN: Eubacteria
(No. 20) PEP FILE: braja.pep ORGANISM: <i>Bradyrhizobium japonicum</i> ; B japonicum; braja DOMAIN: Eubacteria

(No. 21) PEP FILE: brume.pep ORGANISM: Brucella melitensis; B melitensis; brume DOMAIN: Eubacteria
(No. 22) PEP FILE: bucai.pep ORGANISM: Buchnera aphidicola (subsp. Acyrthosiphon pisum); B aphidicola (subsp. Acyrthosiphon pisum); bucai DOMAIN: Eubacteria
(No. 23) PEP FILE: bucap.pep ORGANISM: Buchnera aphidicola (subsp. Schizaphis graminum); B aphidicola (subsp. Schizaphis graminum); bucap DOMAIN: Eubacteria
(No. 24) PEP FILE: bucbp.pep ORGANISM: Buchnera aphidicola (subsp. Baizongia pistaciae); B aphidicola (subsp. Baizongia pistaciae); bucbp DOMAIN: Eubacteria
(No. 25) PEP FILE: caeel.pep ORGANISM: Caenorhabditis elegans; C elegans; caeel DOMAIN: Eukaryote
(No. 26) PEP FILE: camje.pep ORGANISM: Campylobacter jejuni; C jejuni; camje DOMAIN: Eubacteria
(No. 27) PEP FILE: canbf.pep ORGANISM: Candidatus Blochmannia floridanus; C Blochmannia floridanus; canbf DOMAIN: Eubacteria
(No. 28) PEP FILE: caucr.pep ORGANISM: Caulobacter crescentus; C crescentus; caucr DOMAIN: Eubacteria
(No. 29) PEP FILE: chlcv.pep ORGANISM: Chlamydophila caviae; C caviae; chlcv DOMAIN: Eubacteria
(No. 30) PEP FILE: chlmu.pep ORGANISM: Chlamydia muridarum; C muridarum; chlmu DOMAIN: Eubacteria

(No. 31) PEP FILE: chlte.pep ORGANISM: Chlorobium tepidum; C tepidum; chlte DOMAIN: Eubacteria
(No. 32) PEP FILE: chltr.pep ORGANISM: Chlamydia trachomatis; C trachomatis; chltr DOMAIN: Eubacteria
(No. 33) PEP FILE: chrvo.pep ORGANISM: Chromobacterium violaceum ATCC 12472; C violaceum ATCC 12472; chrvo DOMAIN: Eubacteria
(No. 34) PEP FILE: cloab.pep ORGANISM: Clostridium acetobutylicum; C acetobutylicum; cloab DOMAIN: Eubacteria
(No. 35) PEP FILE: clope.pep ORGANISM: Clostridium perfringens; C perfringens; clope DOMAIN: Eubacteria
(No. 36) PEP FILE: clote.pep ORGANISM: Clostridium tetani; C tetani; clote DOMAIN: Eubacteria
(No. 37) PEP FILE: cordi.pep ORGANISM: Corynebacterium diphtheriae NCTC 13129; C diphtheriae NCTC 13129; cordi DOMAIN: Eubacteria
(No. 38) PEP FILE: coref.pep ORGANISM: Corynebacterium efficiens; C efficiens; coref DOMAIN: Eubacteria
(No. 39) PEP FILE: corgl.pep ORGANISM: Corynebacterium glutamicum; C glutamicum; corgl DOMAIN: Eubacteria
(No. 40) PEP FILE: coxbu.pep ORGANISM: Coxiella burnetii; C burnetii; coxbu DOMAIN: Eubacteria

(No. 41) PEP FILE: deira.pep ORGANISM: <i>Deinococcus radiodurans</i> ; D radiodurans; deira DOMAIN: Eubacteria
(No. 42) PEP FILE: desvh.pep ORGANISM: <i>Desulfovibrio vulgaris</i> subsp. <i>vulgaris</i> str. Hildenborough; D vulgaris subsp. <i>vulgaris</i> str. Hildenborough; desvh DOMAIN: Eubacteria
(No. 43) PEP FILE: drome.pep ORGANISM: <i>Drosophila melanogaster</i> ; D melanogaster; drome DOMAIN: Eukaryote
(No. 44) PEP FILE: ecoli.pep ORGANISM: <i>Escherichia coli</i> ; E coli; ecoli DOMAIN: Eubacteria
(No. 45) PEP FILE: entfa.pep ORGANISM: <i>Enterococcus faecalis</i> ; E faecalis; entfa DOMAIN: Eubacteria
(No. 46) PEP FILE: erwca.pep ORGANISM: <i>Erwinia carotovora</i> ; E carotovora; erwca DOMAIN: Eubacteria
(No. 47) PEP FILE: fusnu.pep ORGANISM: <i>Fusobacterium nucleatum</i> ; F nucleatum; fusnu DOMAIN: Eubacteria
(No. 48) PEP FILE: glovi.pep ORGANISM: <i>Gloeobacter violaceus</i> ; G violaceus; glovi DOMAIN: Eubacteria
(No. 49) PEP FILE: haedu.pep ORGANISM: <i>Haemophilus ducreyi</i> ; H ducreyi; haedu DOMAIN: Eubacteria
(No. 50) PEP FILE: haein.pep ORGANISM: <i>Haemophilus influenzae</i> ; H influenzae; haein DOMAIN: Eubacteria

(No. 51) PEP FILE: haln1.pep ORGANISM: Halobacterium sp. (strain NRC-1); H sp. (strain NRC-1); haln1 DOMAIN: Archaeobacteria
(No. 52) PEP FILE: hcmva.pep ORGANISM: Human cytomegalovirus (strain AD169); HCMV (strain AD169); hcmva DOMAIN: virus
(No. 53) PEP FILE: helhe.pep ORGANISM: Helicobacter heilmannii; H heilmannii; helhe DOMAIN: Eubacteria
(No. 54) PEP FILE: helpy.pep ORGANISM: Helicobacter pylori; H pylori; helpy DOMAIN: Eubacteria
(No. 55) PEP FILE: human.pep ORGANISM: Homo sapiens; H sapiens; human DOMAIN: Eukaryote
(No. 56) PEP FILE: lacjo.pep ORGANISM: Lactobacillus johnsonii; L johnsonii; lacjo DOMAIN: Eubacteria
(No. 57) PEP FILE: lacla.pep ORGANISM: Lactococcus lactis (subsp. lactis); L lactis (subsp. lactis); lacla DOMAIN: Eubacteria
(No. 58) PEP FILE: lacpl.pep ORGANISM: Lactobacillus plantarum WCFS1; L plantarum WCFS1; lacpl DOMAIN: Eubacteria
(No. 59) PEP FILE: leixx.pep ORGANISM: Leifsonia xyli (subsp. xyli); L xyli (subsp. xyli); leixx DOMAIN: Eubacteria
(No. 60) PEP FILE: lepic.pep ORGANISM: Leptospira interrogans (serogroup Icterohaemorrhagiae / serovar Copenhageni); L interrogans (serogroup Icterohaemorrhagiae / serovar Copenhageni); lepic DOMAIN: Eubacteria

(No. 61) PEP FILE: lisin.pep ORGANISM: Listeria innocua; L innocua; lisin DOMAIN: Eubacteria
(No. 62) PEP FILE: lismo.pep ORGANISM: Listeria monocytogenes; L monocytogenes; lismo DOMAIN: Eubacteria
(No. 63) PEP FILE: metac.pep ORGANISM: Methanosarcina acetivorans; M acetivorans; metac DOMAIN: Archaeobacteria
(No. 64) PEP FILE: metka.pep ORGANISM: Methanopyrus kandleri; M kandleri; metka DOMAIN: Archaeobacteria
(No. 65) PEP FILE: metth.pep ORGANISM: Methanobacterium thermoautotrophicum; M thermoautotrophicum; metth DOMAIN: Archaeobacteria
(No. 66) PEP FILE: mettm.pep ORGANISM: Methanobacterium thermoautotrophicum; M thermoautotrophicum ; mettm DOMAIN: Archaeobacteria
(No. 67) PEP FILE: mouse.pep ORGANISM: Mus musculus; M musculus; mouse DOMAIN: Eukaryote
(No. 68) PEP FILE: muhv4.pep ORGANISM: Murine herpesvirus 68 strain WUMS; Murine herpesvirus 68 strain WUMS; muhv4 DOMAIN: virus
(No. 69) PEP FILE: mycav.pep ORGANISM: Mycobacterium avium; M avium; mycav DOMAIN: Eubacteria
(No. 70) PEP FILE: mycbo.pep ORGANISM: Mycobacterium bovis AF2122/97; M bovis AF2122/97; mycbo DOMAIN: Eubacteria

(No. 71) PEP FILE: mycga.pep ORGANISM: Mycoplasma gallisepticum; M gallisepticum; mycga DOMAIN: Eubacteria
(No. 72) PEP FILE: mycge.pep ORGANISM: Mycoplasma genitalium; M genitalium; mycge DOMAIN: Eubacteria
(No. 73) PEP FILE: mycms.pep ORGANISM: Mycoplasma mycoides (subsp. mycoides SC); M mycoides (subsp. mycoides SC); mycms DOMAIN: Eubacteria
(No. 74) PEP FILE: mycpn.pep ORGANISM: Mycoplasma pneumoniae; M pneumoniae; mycpn DOMAIN: Eubacteria
(No. 75) PEP FILE: mycpu.pep ORGANISM: Mycoplasma pulmonis; M pulmonis; mycpu DOMAIN: Eubacteria
(No. 76) PEP FILE: neime.pep ORGANISM: Neisseria meningitidis; N meningitidis; neime DOMAIN: Eubacteria
(No. 77) PEP FILE: niteu.pep ORGANISM: Nitrosomonas europaea; N europaea; niteu DOMAIN: Eubacteria
(No. 78) PEP FILE: oceih.pep ORGANISM: Oceanobacillus iheyensis; O iheyensis; oceih DOMAIN: Eubacteria
(No. 79) PEP FILE: porgi.pep ORGANISM: Porphyromonas gingivalis; P gingivalis; porgi DOMAIN: Eubacteria
(No. 80) PEP FILE: pseae.pep ORGANISM: Pseudomonas aeruginosa; P aeruginosa; pseae DOMAIN: Eubacteria

(No. 81) PEP FILE: psepυ.pep ORGANISM: Pseudomonas putida; P putida; psepυ DOMAIN: Eubacteria
(No. 82) PEP FILE: pyrab.pep ORGANISM: Pyrococcus abyssi; P abyssi; pyrab DOMAIN: Archaeobacteria
(No. 83) PEP FILE: pyrfu.pep ORGANISM: Pyrococcus furiosus; P furiosus; pyrfu DOMAIN: Archaeobacteria
(No. 84) PEP FILE: pyrho.pep ORGANISM: Pyrococcus horikoshii; P horikoshii; pyrho DOMAIN: Archaeobacteria
(No. 85) PEP FILE: ralso.pep ORGANISM: Ralstonia solanacearum; R solanacearum; ralso DOMAIN: Eubacteria
(No. 86) PEP FILE: rhilo.pep ORGANISM: Rhizobium loti; R loti; rhilo DOMAIN: Eubacteria
(No. 87) PEP FILE: riccn.pep ORGANISM: Rickettsia conorii; R conorii; riccn DOMAIN: Eubacteria
(No. 88) PEP FILE: schpo.pep PEP FILE: SPBC839_05c ORG Schizosaccharomyces pombe; S pombe; schpo DOMAIN: Eukaryote
(No. 89) PEP FILE: shifl.pep ORGANISM: Shigella flexneri; S flexneri; shifl DOMAIN: Eubacteria
(No. 90) PEP FILE: staaυ.pep ORGANISM: Staphylococcus aureus; S aureus; staaυ DOMAIN: Eubacteria

(No. 91) PEP FILE: strag.pep ORGANISM: Streptococcus agalactiae; S agalactiae; strag DOMAIN: Eubacteria
(No. 92) PEP FILE: strco.pep ORGANISM: Streptomyces coelicolor; S coelicolor; strco DOMAIN: Eubacteria
(No. 93) PEP FILE: strpn.pep ORGANISM: Streptococcus pneumoniae; S pneumoniae; strpn DOMAIN: Eubacteria
(No. 94) PEP FILE: strpy.pep ORGANISM: Streptococcus pyogenes; S pyogenes; strpy DOMAIN: Eubacteria
(No. 95) PEP FILE: sulso.pep ORGANISM: Sulfolobus solfataricus; S solfataricus; sulso DOMAIN: Archaeobacteria
(No. 96) PEP FILE: theac.pep ORGANISM: Thermoplasma acidophilum; T acidophilum; theac DOMAIN: Archaeobacteria
(No. 97) PEP FILE: thema.pep ORGANISM: Thermotoga maritima; T maritima; thema DOMAIN: Eubacteria
(No. 98) PEP FILE: trepa.pep ORGANISM: Treponema pallidum; T pallidum; trepa DOMAIN: Eubacteria
(No. 99) PEP FILE: ureur.pep ORGANISM: Ureaplasma urealyticum; U urealyticum; ureur DOMAIN: Eubacteria
(No. 100) PEP FILE: vibch.pep ORGANISM: Vibrio cholerae; V cholerae; vibch DOMAIN: Eubacteria

(No. 101) PEP FILE: vibpa.pep ORGANISM: <i>Vibrio parahaemolyticus</i> RIMD 2210633; <i>V parahaemolyticus</i> RIMD 2210633; vibpa DOMAIN: Eubacteria
(No. 102) PEP FILE: wolsu.pep ORGANISM: <i>Wolinella succinogenes</i> ; <i>W succinogenes</i> ; wolsu DOMAIN: Eubacteria
(No. 103) PEP FILE: xanac.pep ORGANISM: <i>Xanthomonas axonopodis</i> (pv. citri); <i>X axonopodis</i> (pv. citri); xanac DOMAIN: Eubacteria
(No. 104) PEP FILE: xylfa.pep ORGANISM: <i>Xylella fastidiosa</i> ; <i>X fastidiosa</i> ; xylfa DOMAIN: Eubacteria
(No. 105) PEP FILE: yeast.pep ORGANISM: <i>Saccharomyces cerevisiae</i> ; <i>S cerevisiae</i> ; yeast DOMAIN: Eukaryote
(No. 106) PEP FILE: yerpe.pep ORGANISM: <i>Yersinia pestis</i> ; <i>Y pestis</i> ; yerpe DOMAIN: Eubacteria

Supplementary Table 2: Data of η , θ and the comparison between theoretical predictions and experimental observations for genome size and gene number.

Notes: The serial numbers for organisms here are the same numbers for the organisms in Supplementary Table 1. The data of non-coding DNA contents η and the genome sizes are obtained from Ref. [18], where there are 54 species (6 eukaryotes, 5 archaeobacteria and 43 eubacteria, i.e., 48 prokaryotes in total) can be also found in database PEP. The gene numbers are obtained by the numbers of Open Reading Frames (ORFs) in proteomes in PEP. The non-coding content is obtained according to the Human genome draft in this table according to Ref. [18]. But we choose the more precise value of η^* according to the finished euchromatic sequence of the human genome in Ref. [17] to calculate the accurate time of the Cambrian explosion.

No.	η	θ	genome size	$S(\eta, \theta)$	gene number	$N(\eta, \theta)$
1		0.4960			683	
2		0.2571			3322	
3	0.1088	0.4874	1669695	9.6490e+005	2694	839.3707
4	0.1170	0.2173	5674062	4.7051e+006	5402	4.7732e+003
5		0.2238			5274	
6	0.0700	0.3620	1551335	1.5559e+006	1522	1.7165e+003
7	0.7120	0.2096	115409949	1.8103e+008	25541	1.8126e+004
8	0.0780	0.2996	2178400	2.3277e+006	2406	2.5982e+003
9	0.1590	0.2681	5370060	4.5484e+006	5311	3.7826e+003
10	0.1600	0.2452	546909	5.2118e+006	5274	4.3859e+003
11	0.1300	0.2428	4214810	4.4046e+006	4099	4.1737e+003
12		0.2617			4776	
13		0.3886			1482	
14		0.4112			1141	
15		0.2575			3584	
16		0.2649			4986	
17	0.0630	0.4649	1443725	8.3102e+005	850	877.8284
18		0.2744			4184	
19		0.6183			3446	
20		0.1805			8307	
21	0.1300	0.3146	3294935	2.9287e+006	2059	2.6414e+003
22	0.1640	0.5060	618000	1.2136e+006	574	840.3921
23	0.1700	0.5028	640000	1.2814e+006	546	868.7162
24		0.5092			504	
25	0.7419	0.1945	97000000	2.3647e+008	21832	2.1291e+004
26	0.0570	0.3441	1641181	1.5915e+006	1633	1.8700e+003
27		0.5105			583	
28	0.0940	0.2471	4016942	3.4556e+006	3737	3.7569e+003
29		0.4177			998	
30		0.4590			907	
31	0.1110	0.4107	2154946	1.5126e+006	2252	1.3753e+003
32		0.4502			894	
33	0.1100	0.2228	4751080	4.3729e+006	4396	4.5420e+003
34	0.1200	0.2442	3940880	4.1134e+006	3847	4.0489e+003
35	0.1690	0.2695	3031430	4.7935e+006	2722	3.8301e+003
36		0.3379			2373	
37		0.2937			2269	
38		0.2943			2947	
39		0.2645			2989	
40	0.1100	0.4060	1995275	1.5434e+006	2009	1.4133e+003

No.	η	θ	genome size	$S(\eta, \theta)$	gene number	$N(\eta, \theta)$
41	0.0910	0.2753	3284156	2.8916e+006	3099	3.1197e+003
42		0.3107			3524	
43	0.8100	0.2562	120000000	2.5164e+008	18358	1.6650e+004
44	0.1220	0.2247	4641000	4.6505e+006	4281	4.6032e+003
45	0.1200	0.2852	3218031	3.2588e+006	3145	3.1186e+003
46		0.2226			4463	
47	0.1020	0.3149	2714500	2.4678e+006	2067	2.4821e+003
48		0.2462			4425	
49		0.4102			1715	
50	0.1500	0.3434	4524893	2.8080e+006	1709	2.2966e+003
51		0.3185			2058	
52		0.6795			202	
53	0.0700	0.3495	1799146	1.6699e+006	1874	1.8581e+003
54	0.0920	0.3633	1643831	1.7640e+006	1564	1.7844e+003
55	0.9830	0.1889	3.0000e+009	1.0522e+009	37229	3.7131e+004
56		0.3399			1813	
57	0.1260	0.3358	2365589	2.5342e+006	2266	2.2879e+003
58		0.2637			3002	
59		0.3320			2023	
60		0.2837			3652	
61	0.0970	0.2748	3011209	3.0073e+006	2968	3.1706e+003
62	0.0970	0.2622	2944528	3.2293e+006	2833	3.4342e+003
63		0.2999			4540	
64		0.3418			1687	
65	0.0800	0.3228	1751377	2.0652e+006	1873	2.2511e+003
66		0.3222			1869	
67	0.9500	0.1828	2.5000e+009	8.9214e+008	28085	3.5960e+004
68		0.8092			80	
69		0.2537			4340	
70	0.0900	0.2451	4345492	3.4112e+006	3906	3.7721e+003
71		0.5086			726	
72	0.1200	0.5416	580070	7.5934e+005	484	609.2149
73		0.5674			1016	
74		0.4804			686	
75	0.0860	0.4867	963879	8.4373e+005	778	802.6126
76	0.1710	0.3407	2184406	3.2388e+006	2065	2.4452e+003
77		0.3436			2461	
78		0.2513			3496	
79		0.3800			1909	
80	0.1060	0.2167	6264403	4.4184e+006	5563	4.6810e+003

No.	η	θ	genome size	$S(\eta, \theta)$	gene number	$N(\eta, \theta)$
81		0.2240			5316	
82		0.3236			1764	
83		0.3071			2065	
84	0.1320	0.3851	6397126	1.9863e+006	2064	1.6935e+003
85	0.1270	0.2242	5810922	4.8078e+006	5092	4.6687e+003
86		0.1953			7264	
87	0.1900	0.5019	1268755	1.4540e+006	1374	912.3452
88	0.4250	0.3018	13800000	1.8831e+007	4987	5.4215e+003
89		0.4419			4176	
90	0.1690	0.2845	2878084	4.4024e+006	2631	3.4816e+003
91		0.3210			2121	
92	0.1110	0.1809	8670000	5.5793e+006	7894	5.9409e+003
93		0.3949			2094	
94		0.3350			1845	
95		0.3006			2977	
96	0.1300	0.3378	1564905	2.5671e+006	1478	2.2787e+003
97	0.0500	0.3316	1860725	1.6375e+006	1846	1.9943e+003
98	0.1280	0.4457	1900521	1.3744e+006	1031	1.1417e+003
99	0.0700	0.5053	751719	6.8918e+005	611	688.9768
100	0.1255	0.3336	4034065	2.5593e+006	2736	2.3187e+003
101		0.2561			4800	
102	0.0600	0.3362	2110355	1.6949e+006	2044	1.9790e+003
103	0.1440	0.2545	5175554	4.4875e+006	4029	3.9940e+003
104	0.1200	0.4376	2679305	1.3711e+006	2763	1.1815e+003
105		0.3221			6356	
106	0.1420	0.3265	4653728	2.9448e+006	4087	2.5139e+003